

# Automated Laser Ultrasonic Testing (ALUT) of Hybrid Arc Welds for Pipeline Construction, #272

**DOT OTA No. DTPH56-07-T-000008**

## **Final Report**

December 22, 2009

Period of Performance: 08/01/07 to 11/30/09

*Sponsor:*

DOT/PHMSA  
Washington, DC

*Technical Monitor:*

James Merritt  
303-683-3117

*Presented by:*

Intelligent Optical Systems, Inc.  
2520 West 237th Street  
Torrance, California 90505

*Principal Investigator*

Marvin Klein, Ph.D.  
424-263-6361

---

*The information in this report, and any hardware delivered, is the property of Intelligent Optical Systems, Inc., as set forth in Article I, Section C, Paragraph 4 of the OTA DTPH56-07-T-000008 (#272).*

---

## TABLE OF CONTENTS

ATTACHMENT 1 .....	2
Technical Status, Results, and Conclusions.....	2
1.0 INTRODUCTION .....	2
2.0 CURRENT STATE OF THE ART AND PROJECT OBJECTIVES .....	3
3.0 TECHNICAL APPROACH.....	4
4.0 TASK DESCRIPTION .....	4
5.0 INTRODUCTION TO INSPECTION APPROACH .....	6
6.0 RESULTS OF THIS PROJECT .....	8
6.1 <i>Task 1: System Engineering</i> .....	8
6.1.1 Development of System Specification.....	8
6.1.2 Initial ROI Analysis .....	9
6.2 <i>Task 2: Implementation of System Improvements</i> .....	9
6.2.1 Measurements on Root Pass Weld.....	9
6.3 <i>Task 3: Validation Tests</i> .....	10
6.3.1 Testing of Simulated and HLAW Welds .....	10
6.3.2 Finite Difference Simulations .....	13
6.4 <i>Task 4: Phase I Project Administration and Reporting</i> .....	15
6.5 <i>Task 5: Integration for Remote Testing</i> .....	15
6.5.1 Integration Activities at IOS .....	15
6.5.3 High Power Probe Laser Design Modified.....	16
6.5.4 Receiver Modifications Complete .....	17
6.6 <i>Task 6: Evaluation and Qualification at BMT</i> .....	17
6.6.1 Benchmarking against Phased Array UT.....	17
6.6.2 Demo of ALUT System with HLAW Demo .....	19
6.7 <i>Task 7: Develop Final System Specification</i> .....	22
6.8 <i>Task 8: Update ROI Analysis</i> .....	22
6.9 <i>Task 9: Phase II Project Administration and Reporting</i> .....	23
ATTACHMENT 2 .....	24

## ATTACHMENT 1

### Technical Status, Results, and Conclusions

#### 1.0 INTRODUCTION

One challenge in developing new gas reserves is the high cost of pipeline construction. Welding costs are a major component of overall construction costs. Industry continues to seek advanced pipeline welding technologies to improve productivity and save money. The current state-of-the-art welding processes for onshore pipelines involve mechanized gas metal arc welding (GMAW). Based on recent improvements of weld lasers and laser welding technology, the next generation of automated pipeline welding equipment probably will be built around hybrid laser arc welding (HLAW), which has many benefits, including lower joint preparation costs, reduced filler metal requirements, smaller weld bead volume, higher weld speed, and less susceptibility to hydrogen cracking; there is also a small grain size heat-affected zone with improved toughness. A higher degree of automation will reduce labor and repair costs. Successful achievement of the HLAW system development will reduce the cost of fabricating girth welds in high strength steel pipelines, and more importantly, ensure their in-service integrity and safety.

As the HLAW technique is developed and implemented for pipeline construction, it is important to develop an associated technique for weld inspection. Currently, the most popular technique for inspection of new pipeline welds is phased array ultrasonic testing (PAUT), which is reaching technological maturity and has been commercialized by several companies. However, phased arrays require a couplant of either flowing water or a related liquid; the couplant limits PAUT to post-process applications. The delayed inspection of new welds enables the detection of delayed cracking. However, the HLAW approach in high strength steel is much less likely to produce delayed cracking, providing the opportunity to integrate inspection technologies during the weld process. Productivity increases through early detection of defects allows repairs on a per-pass basis and adjustments of process parameters to help limit these defects.

This report describes a program for developing, testing, and validating in-process automated laser ultrasonic testing (ALUT) of new HLAW welds in the field. The goal of the project is to apply the proven technologies of laser ultrasonics and modern signal processing techniques to the important problem of evaluating HLAW pipeline welds in high strength steel pipelines. Laser ultrasonic testing (LUT) offers the advantage of true in-process measurement, providing immediate information on weld integrity. As conceived in this application, a small fiber-delivered measurement head would be mounted in tandem with the weld head, so that testing can be performed immediately after the weld is formed. This process monitor function will enable immediate inspection on a per-pass basis and also save the cost of equipment and crew used in post-process inspection. More important, repair costs will be significantly reduced. LUT is a true noncontact technique, with no liquid couplant and a standoff from the pipe surface that can reach up to approximately 0.5 m. LUT can perform measurements at surface speeds far above those used in girth welding. Another major benefit of laser ultrasonics is that the laser beams on the surface are typically 0.1 mm; therefore, spatial resolution is high, and access to tight spaces is enabled. Finally, the measurement bandwidth is typically 50 MHz in a short pulse, providing high depth resolution and high information content in the detected waves. Laser generation

produces a rich admixture of ultrasonic waves, covering many wave types, directions, and frequencies.

This project was part of a consolidated program led by BMT Fleet Technology that includes a separate project to develop the HLAW process for pipeline welding. The joint efforts of the two teams have been able to accelerate the insertion and acceptance of the HLAW approach for girth welding in new pipelines.

## **2.0 CURRENT STATE OF THE ART AND PROJECT OBJECTIVES**

Pipeline in-service integrity and safety is clearly dependent on identifying and repairing defects in new welds before the pipeline is put into service. Because pipeline girth welds must undergo stringent inspections governed by established codes, the accurate detection, positioning, and sizing of defects will allow the wider use of engineering critical assessment (ECA).

As mentioned previously, any inspection technique for girth welds in onshore pipelines must be able to detect, position, and size internal anomalies, most importantly planar defects, such as lack of fusion and cracks. A typical requirement for conventional automated ultrasonic testing (AUT) defects is that *those greater than 1 mm in through wall height and longer than 6 mm should be detectable within the accepted industry standard of probability of detection (POD) at 90% with a confidence level of 95%*, a requirement sometimes called the 90/95% rule.

Automated inspection based on AUT is now in common use. Ultrasonic testing (UT) must be able to deal with many challenges, including material anisotropy and temperature variations that affect wave velocity and directionality, as well as the requirement to focus beams to individual regions of interest and the unknown shape, size, orientation, and position of the anomaly. Early AUT systems were based on the use of multiple transducers at fixed positions on both sides of the weld seam, typically operating in the pulse echo or pitch-catch configuration. The weld bead is divided into zones in depth with a height of a few millimeters. Each transducer or transducer pair is dedicated to the inspection of a particular zone, using beams that are directed to that zone. All the transducers generate angled beams, sometimes with one or two skips. The amplitude of the reflected wave frequently gives information about the size of the defect. These systems sometimes offer the added capability of performing time of flight diffraction (TOFD) measurements, which help considerably in determining the depth and height of the defect. All AUT systems require coupling to the surface using a constant flow of fluid couplant.

Recently, phased array systems have become more popular. These systems include a one-dimensional array of transducers that focus and scan one or more separate waves through proper timing of each transducer. The largest commercial vendor of phased array systems for inspection of pipeline girth welds is Olympus NDT, which was a participant in this project.

As with all transducer-based ultrasonic systems, phased arrays require a fluid couplant, which adds hardware complexity and makes it impossible to run in tandem with the weld process. The pan or phased array probe that is in contact with the pipe is typically 2 in or greater. Each pipe diameter and wall thickness requires a separate probe setup. The requirement for precision probes and separate channels for each individual transducer complicates signal interpretation and adds complexity and cost. In spite of great efforts in the testing industry to meet inspection requirements, POD and confidence values are not at adequate levels. In fact, several benchmark studies have shown great variation in results between separate systems.

In summary, current girth weld AUT systems are intrinsically post-process, require complex probes with multiple transducers (and/or beam scanning), have limited sensitivity near the OD and ID surfaces and, in general, fall short in meeting inspection requirements for POD and confidence level. From a signal processing point of view, the typical transducer frequency, 5 MHz or 7.5 MHz, implies a limited frequency bandwidth, which limits the accuracy of the arrival time measurements that defect sizing requires.

The work in this project addressed the previously-mentioned gaps to provide an in-process ALUT system with a simple optical probe that delivers a minimal number of laser beams to the pipe surface. The projected inspection performance will provide higher POD than transducer-based and phased array UT at all defect depths, but with the benefit of real time data on a per-pass basis that can be used to control the weld parameters. These innovations will reduce labor and repair costs and enhance pipeline safety.

This project had the following technical objectives:

- To implement improvements to each of the three major hardware components so as to produce improvement in the signal-to-noise ratio (SNR) and the depth of field,
- To develop the beam configuration on the pipe surface that optimizes detection and sizing accuracy, especially near the ID and OD surfaces,
- To introduce new signal processing techniques,
- To validate the system in tests on real pipe welds,
- To benchmark the results against state-of-the-art PAUT, and
- To develop final system specifications, a Users' Guide and an ROI calculation.

### **3.0 TECHNICAL APPROACH**

While the broad benefits of laser ultrasonics are well known and a number of applications have been developed, the use of this technique for detecting and sizing relatively small and deep defects has been limited by insufficient capability for measuring weak signal arrivals in the presence of significant background noise. Therefore, a main objective of our technical efforts was to enhance the SNR for the specific requirements of this project. IOS sought to implement improvements in instrument performance and beam placement on the pipe surface, and to increase values of laser power and energy. Equally important, we applied a number of modern signal processing techniques, which we believe provide great potential for SNR improvement for girth weld inspection.

### **4.0 TASK DESCRIPTION**

In this project, we have built on lessons learned in related DOT co-funded projects and other application studies to develop the ALUT technique for process monitoring of HLAW welds. The co-development and insertion of the HLAW and ALUT technologies will enable a major enhancement of the productivity and integrity of full circumferential girth welding while reducing inspection and repair costs.

At each stage of the project, team members and their industry sponsors on the companion project met to guide the ALUT strategy. The major milestone in this project was a demonstration of an ALUT system integrated into the HLAW weld head.

The following paragraphs describe the tasks for this project. The tasks were established and timed to coordinate with tasks in the related project on HLAW girth weld development.

*Task 1. System Engineering*

Consult with partners in the HLAW project and their co-funding sponsors to develop a performance specification for the ALUT subsystem that covers mechanical, electrical, and optical integration into a full HLAW system. Based on these specifications, work with the HLAW team to develop a full system design that will be enabled through the use of solid modeling such as SolidWorks. This model will be versatile enough to accommodate modifications and improvements to subsystems as the projects progress. The system design will include provision for laser eye safety protection as determined by industry codes. Finally perform a preliminary ROI analysis.

*Task 2. Implementation of System Improvements*

Extend the capability of our current technology to sensing defects at depths consistent with the expected wall thickness. This effort covered several areas, including hardware improvements and signal conditioning and processing implementation.

Hardware improvements to be implemented include (1) the design of a specialized beam delivery head for integration with the weld head, (2) adapting current fiber beam delivery systems to allow multiplexed delivery of a tone burst from the generation laser, and (3) enhancing the receiver SNR through cooling of the photodiode detector. As these developments proceed, it will be necessary to determine the size, shape, and position of the beams for highest accuracy in detecting, locating, and sizing defects.

The signal processing efforts are focused on techniques to identify the appropriate arrivals and make an accurate calculation of amplitude and arrival time. At the end of this task, a full breadboard will be available for the testing in Task 3.

*Task 3. Validation Tests*

The first step is to fabricate test blocks containing simulated defects over a range of depths. The material for these blocks should be the same as used in current new pipelines. The next step is to obtain HLAW weld coupons with intentional (and characterized) defects, as these samples become available. In each case, it will be necessary to determine the capability to detect defects and measure their size and depth. Upon completion of the tests on HLAW welds, the samples will be sectioned and the ALUT measurements will be compared with macro results.

*Task 4. Phase I Project Administration and Reporting*

Prepare monthly and quarterly, reports, summarizing the results of the project efforts and reporting milestone results. Regular coordination meetings with the HLAW team and co-funders are necessary to provide guidance to this project and enable effective integration of the two systems.

*Task 5. Integration for Remote Testing*

In this task, the breadboard developed and assembled for testing during Phase I will be hardened for integration and testing at BMT. The measurement head will be engineered for mounting on or near the weld head. Controls and user interface required for the ALUT system will be integrated with those for the HLAW system. To the extent possible, this hardened prototype will be tested first at IOS. The final activity in this task will be shipment to BMT and assembly of the integrated system.

*Task 6. Evaluation and Qualification at BMT*

This task covers full scale tests at BMT of the integrated HLAW/ALUT system, producing and monitoring girth welds on pipeline sections. The defect data will be compared with studies of macro sections. The data will also be benchmarked against PAUT data provided by a commercial Olympus system.

*Task 7. Develop Final System Specification and Users Guide*

Upon completion of the tests at BMT, a set of system specifications will be developed and included in the final report. These specifications will be consistent with those provided for the HLAW weld system and will allow a girth weld equipment integrator or end user to purchase or build a proven system and offer it for weld process monitoring. A Users' Guide will also be provided to detail the operation of the ALUT subsystem.

*Task 8. Update Calculation of ROI*

We will determine the sources of cost savings enabled by ALUT and calculate the dollar savings per year over current practice. Current approaches to be considered are discrete transducer-based and phased array systems. The calculated cost savings will be measured against the estimated cost of an ALUT system to determine a payback period.

*Task 9. Phase II Project Administration and Reporting*

Prepare monthly and quarterly reports, as well as a final report, summarizing the results of the project efforts and reporting milestone results. Regular coordination meetings with the HLAW team members and co-funders will provide guidance to this project and enable effective integration of the two systems.

## **5.0 INTRODUCTION TO INSPECTION APPROACH**

We have developed a laser ultrasonic inspection technique that is much simpler than current contact techniques, and is well suited for automated operation. In Figure 1, we show a schematic of our measurement approach. An actual macro of an HLAW weld is overlaid by the laser beams, and shows the paths of the relevant ultrasonic waves. We have used time-of-flight diffraction for the detection of defects, with the arrival time indicating the depth of the defect. Assuming we are using only longitudinal waves, then arrivals associated with defect scattering will always occur before the back wall reflection. The desired arrivals are thus free of any interference from bulk waves. However, as seen in Figure 1, there is a risk of interference from surface waves along the crown or shock waves in air. Thus, there is a window in time when defect arrivals are free of interference. This window varies with the beam separation.

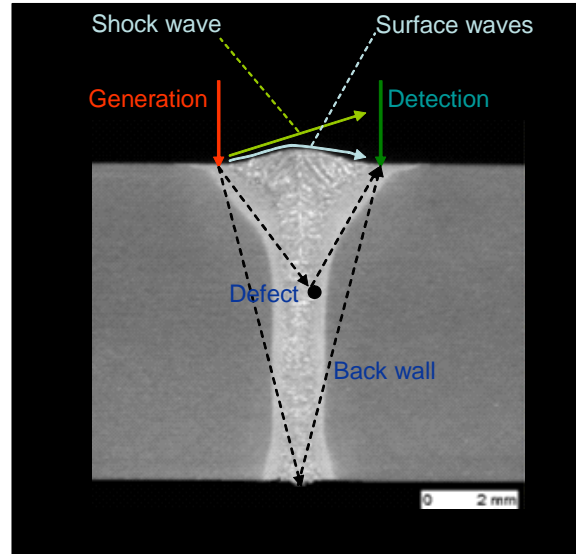


**Figure 1** Schematic of inspection configuration.

In order to understand the detection window for our technique, we performed an experiment on an 18 mm flat sample of X100 material provided by the HLAW team. We varied the beam separation continuously and recorded the temporal signal at each position. The temporal signals were stacked together, with amplitude shown in grey scale, to form a B-scan. This scan is shown in Figure 2. The strong line emanating from the overlap position is a direct Rayleigh wave as shown in Figure 1. The weaker line to the left is a surface-skimming longitudinal wave. The slightly curved line near the center is the back wall reflection. The triangular region at the bottom is associated with the shock wave in air. At each value of beam spacing, there is an arrival time of the Rayleigh wave at which a defect arrival could become lost. For example, at a 6 mm beam spacing, the Rayleigh arrival is at  $\sim 1.9 \mu\text{s}$  (see Figure 3), corresponding to the arrival time of a reflected bulk wave from a defect at  $\sim 5 \text{ mm}$  depth.

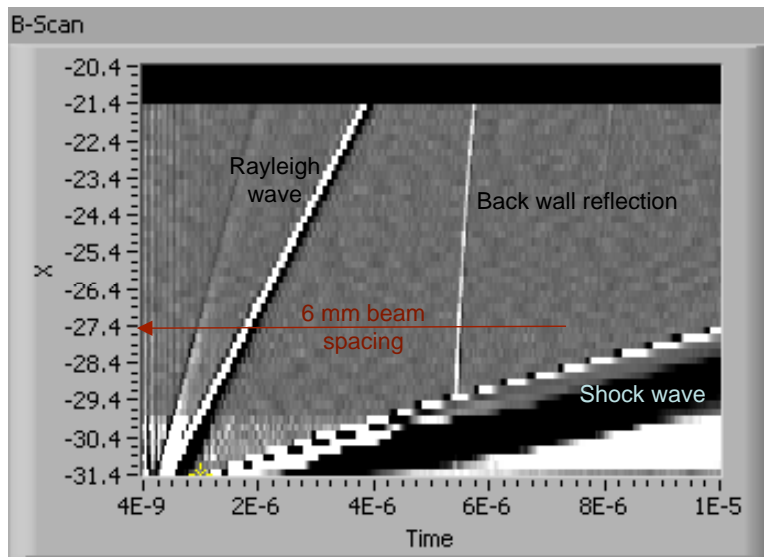


**Figure 2** B-scan on 18 mm thick X100 sample. The vertical scale is beam separation in mm.

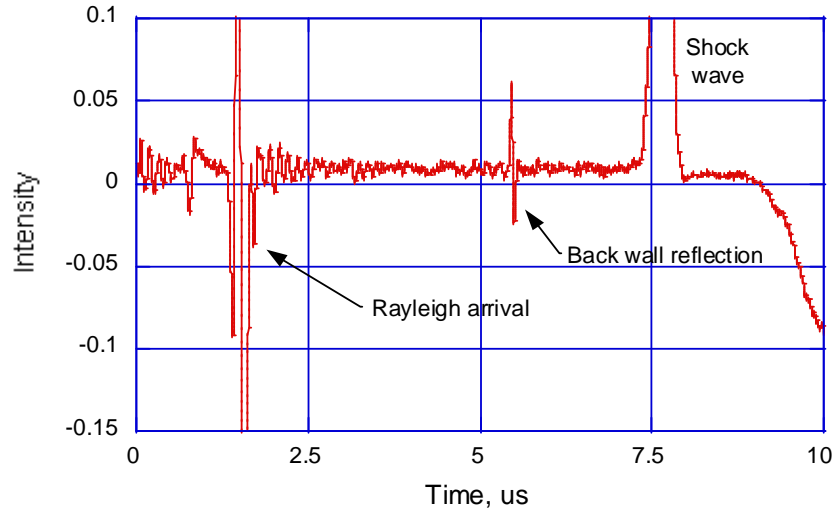


**Figure 3** Temporal signal for a beam separation of 6 mm.

## 6.0 RESULTS OF THIS PROJECT

### 6.1 *Task 1: System Engineering*

#### 6.1.1 Development of System Specification

The critical system specifications cover mechanical integration with the HLAW system and the optical configuration of the laser ultrasonic subsystem.

#### **Mechanical Integration with HLAW System**

We assume first of all that the measurement head will be delivered and scanned with a mechanical stage. It is important to specify the stage in the weld process when the inspection will take place:

- In process, directly behind the weld head. In this case, the measurement head would be integrated with the weld head; and
- Post process, after weld passes are complete. In this case, the measurement head would be used separately from the weld head.

The post process approach is the more likely and preferable one, as there would be no interference from the weld process.

It is also important to specify the positioning of the measurement head relative to the pipe surface. Like all optical systems, the measurement head has a finite depth of focus centered around the standoff distance. It is desirable that this intrinsic optical depth of focus be adequate to compensate for variations encountered during the inspection process. If this is not the case, then we will need to mount the head on surface-conforming wheels or implement autofocus.

#### **Specification of Laser Ultrasonic Configuration, Components and Performance**

The major design decision is the layout of the generation and detection beams. The configuration of Figure 1 is intuitive, but (as discussed above) a single pair of beams will always have a possible blind spot associated with the strong Rayleigh arrival. We expect that finite difference modeling will help determine the optimum beam separation, and determine the effectiveness of more than two beams.

In order to specify the laser ultrasonic system performance, it is critical to know the defect detection requirements related to depth, type and size. The current standard API1104 provides detection criteria related to current inspection practice. A new and different inspection approach such as ours will inevitably require a new standard. We are in continued discussion with inspection experts at TransCanada regarding the physical requirements for defect detection and evaluation.

It is important to establish the required repetition rate for the generation laser, as this has a big impact on laser selection. Based on a measurement speed of 1.2 m/min and a measurement spacing of 1 mm, we require 20 measurements per second. To allow for 5 averages, the laser rep rate is determined to be 100 Hz. There are a number of laser candidates providing up to 20 mJ per pulse at 100 Hz.

### 6.1.2 Initial ROI Analysis

As a first step in calculating ROI, it is necessary to understand the sources of cost savings. We consulted with several HLAW team members, including David Taylor at TransCanada, in order to understand how ALUT is used. The consensus early in the project was that ALUT would be performed on a separate scan along the weld, after the weld passes are complete. In this case, the economic benefits would be:

- Identification of volumetric defects at the time of welding means that repair could be completed while the joint is already enclosed, prepared and pre-heated. This should be faster and less expensive than if the joint needs to be set up again;
- Automated ALUT inspection as an alternative to manual and more expensive ultrasonic and x-ray inspection will lead to reduced labor costs; and
- Alternatively, ALUT may allow inspectors to focus their efforts on questionable weld joints and not spend their time on joints that are clearly free from discontinuities.

## 6.2 Task 2: Implementation of System Improvements

### 6.2.1 Measurements on Root Pass Weld

To study the grain structure in more detail, we performed B-scans on an HLAW sample provided by Precision Light Systems. The material was X80 high strength steel. As shown in Figure 4, the weld consisted of a root pass in 16 mm material. We separated the laser beams by 13 mm, so as to straddle the weld. Scans were made along the weld and on a portion of the sample with no weld.

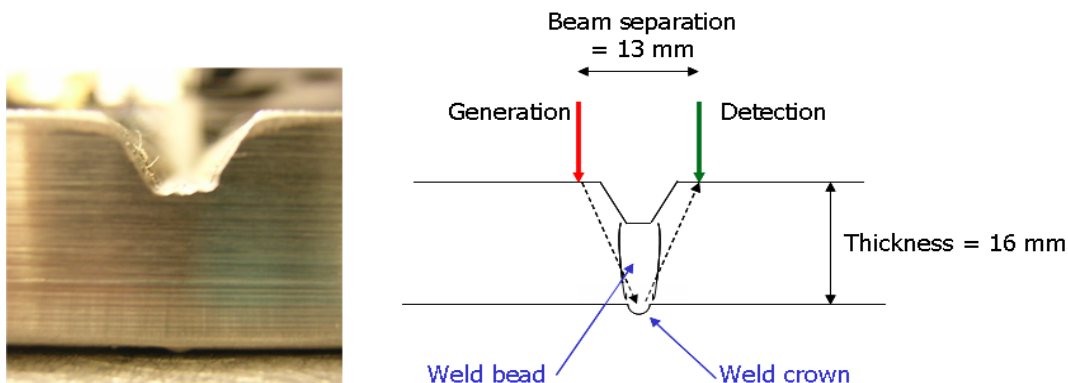


**Figure 4** Photo (left) and setup (right) for scanning of HLAW sample.

B-scans for the above conditions are shown in Figures 5 and 6. With no weld, there is a direct arriving Rayleigh (surface) wave and a clear back wall reflection. When scanning over a weld, the surface wave path is extended, so the arrival moves to a later time. In addition, the weld crown distorts the back wall arrival. We also note that grain scattering in the weld scan is not prominent. This is promising and suggests that signal-to-noise will not be compromised.

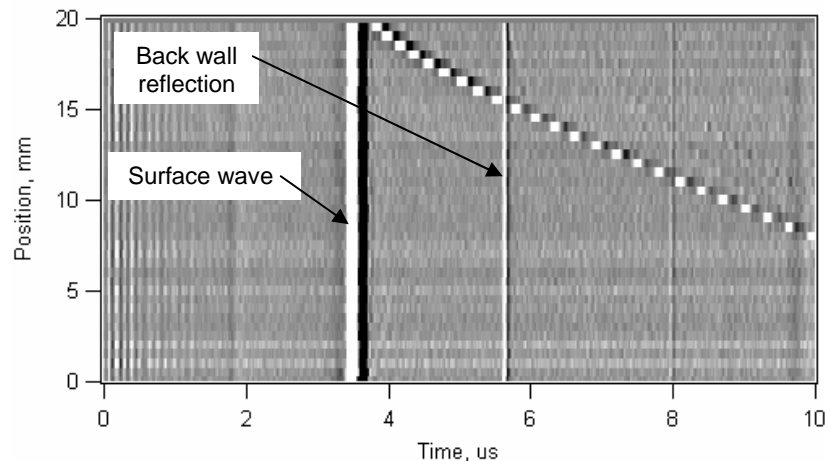


**Figure 5** B-scan over region with no weld.

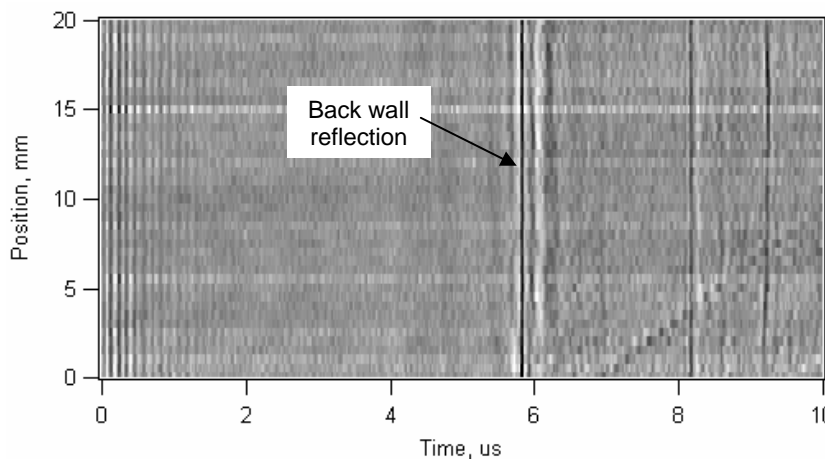


**Figure 6** B-scan over welded region. The surface wave is delayed and the back wall reflected arrival is distorted by the weld crown.

### 6.3 Task 3: Validation Tests

#### 6.3.1 Testing of Simulated and HLAW Welds

As a simulation, we fabricated and tested a sample of X100 steel that had a series of EDM holes and notches produced on one face. In one experiment, we scanned the two beams on the opposite face, with the beams straddling a 2 mm wide notch on the back face that had a depth that tapered from 3 to 9 mm. This configuration is shown in Figure 7. The sample thickness was 16 mm.

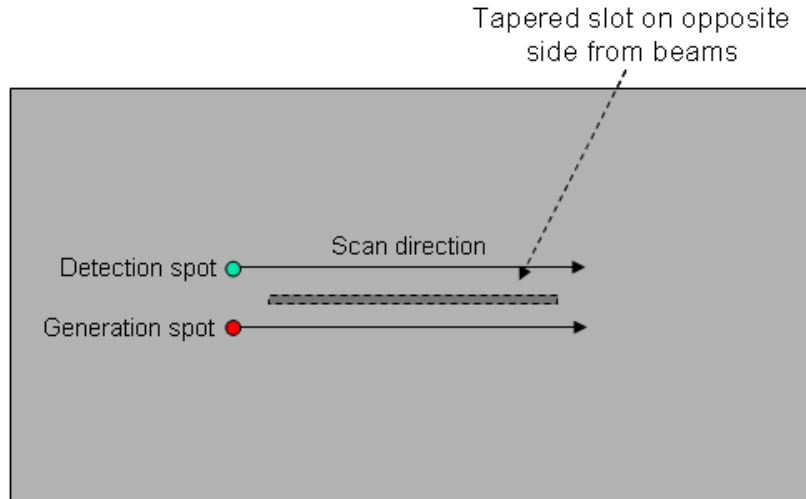


**Figure 7** Beam scan configuration over EDM notch with tapered depth.

A typical B-scan that we obtained is shown in Figure 8. The strong vertical feature at  $\sim 3$   $\mu\text{s}$  arrival time is the direct arriving Rayleigh wave. The slight tilt of this and a later Rayleigh reflection at  $\sim 9$   $\mu\text{s}$  is associated with a small change in beam separation associated with the fixturing of the part.

In Figure 8, the features of interest are the strongly slanted arrivals identified in red. The earlier of the two arrivals is a longitudinal wave reflection from the bottom of the notch. The second arrival is a mode converted (longitudinal/shear wave) reflection. In this basic experiment, the notch is clearly visible, even at a depth of 13 mm.

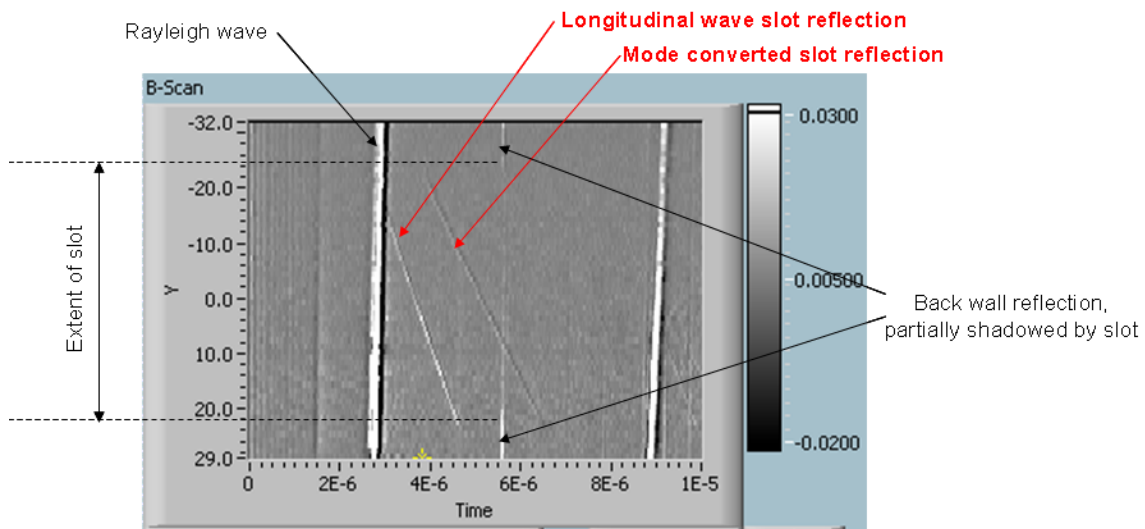


**Figure 8** B-scan along tapered notch.

As a second simulation, we fabricated and tested another steel sample that had a series of EDM holes and notches produced on one face. In one experiment, we scanned the two beams on the opposite face, with the beams passing over three 1 mm wide notches having three different depths. This configuration is shown in Figure 9. The sample thickness was 15 mm.

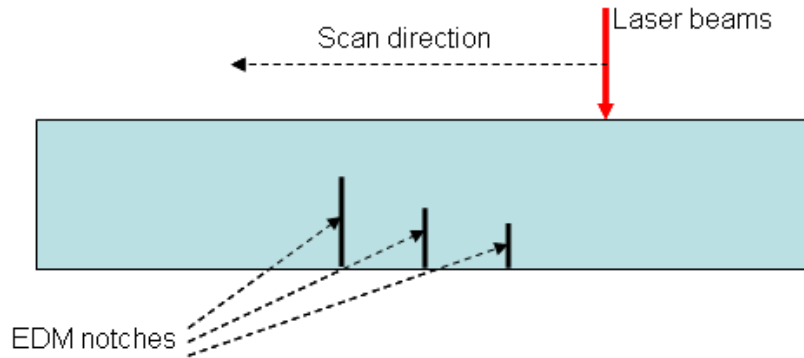
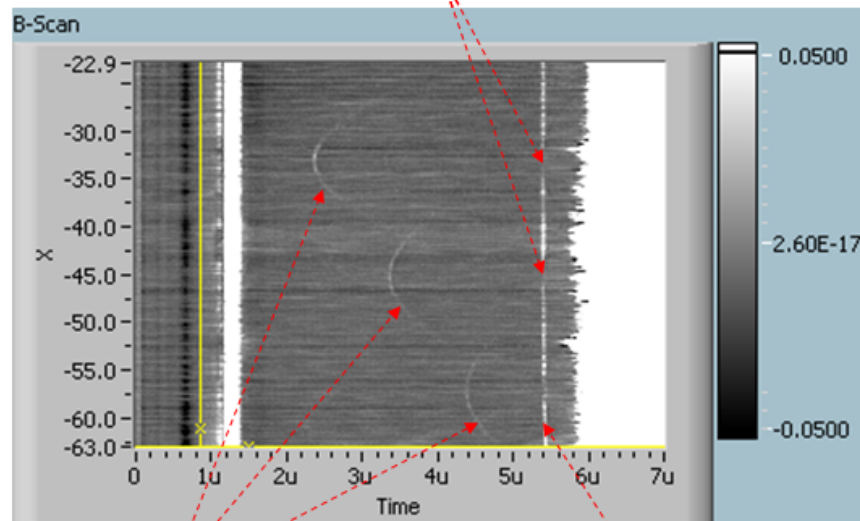


**Figure 9** Beam scan configuration over EDM notches with depths of 3, 6 and 9 mm from the opposite face.

A typical B-scan that we obtained is shown in Figure 10. The strong vertical feature at  $\sim 1.2$  us arrival time is the direct arriving Rayleigh wave. The features of interest are the three parabolic shaped arrivals. The parabolas are very typical of defect reflections using beams that have a finite angular spread. Note that the back wall reflection disappears behind the notches, since the notches extend all the way to the back wall. For a buried defect, the back wall reflection would not disappear.

Back wall reflection disappears at position of notch



Reflection from EDM notches

Back wall reflection

**Figure 10** B-scan across three EDM notches.

Figure 11 shows a processed version of the raw data in Figure 10, in which synthetic aperture techniques have been applied to localize the position of the three notches.

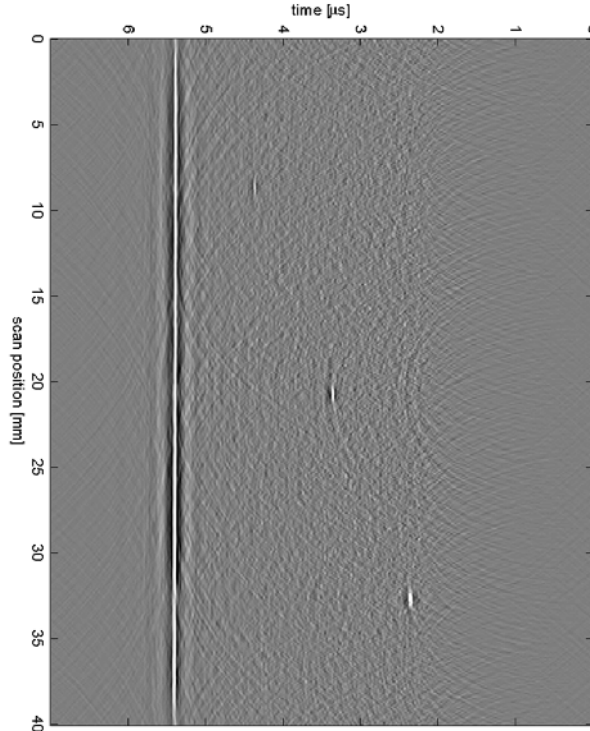


**Figure 11** Processed version of the data plotted in Figure 10, in which the three notches have been localized.

### 6.3.2 Finite Difference Simulations

Simulations and signal processing were conducted by TNO Research and Industry, Delft, Netherlands. The first simulations focused on a series of internal cracks that were perpendicular to the surface. The cracks were positioned at various positions relative to the two sample surfaces. The top surface contained a U-shaped notch indicating the region where a second weld pass will take place. Figures 12-14 show three frames from a video which follows the laser-generated waves as they interact with various features in the sample. In this case, the crack is near the center of the sample. Figure 12 shows the laser-generated waves coming from the top left surface arriving at the crack. In Figure 13, scattering from both the top and bottom of the crack is clearly visible as circular features centered on these two positions. Figure 14 shows a frame at a time when the scattered waves are arriving at the top right surface. It is clear that the crack-related arrivals are difficult to distinguish from the many arrivals associated with normal features of the sample.

One way to avoid interference from unwanted arrivals is to increase the separation between the beams. In the limit of very large beam separation, longitudinal waves scattered from internal cracks will be the first to arrive, and thus cannot suffer any interference from other arrivals. However, beam directionality and beam spreading favor a very small separation between the beams.

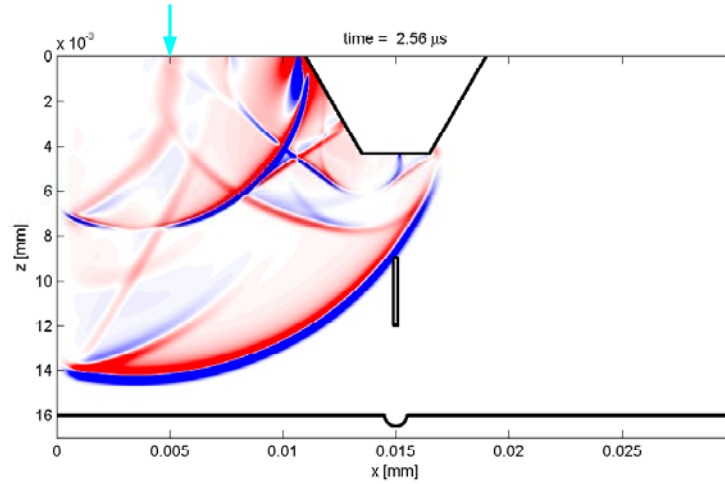


**Figure 12** Wavefront positions 2.56 us after laser generation at the position shown by the arrow.

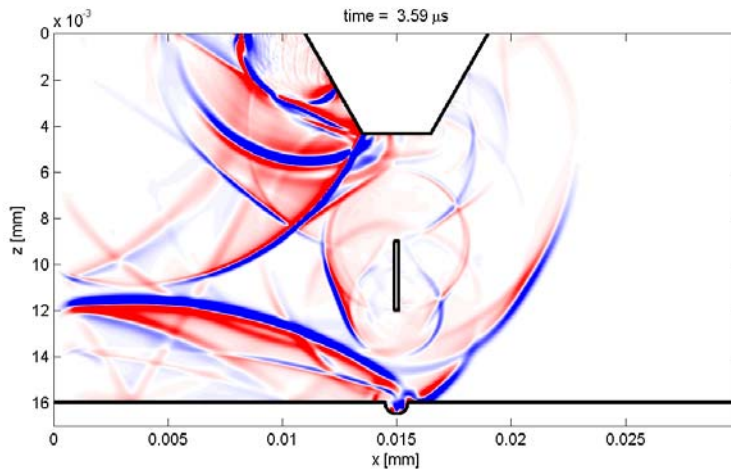


**Figure 13** Wavefront positions 3.59 us after laser generation, showing waves scattering from the top and bottom of the buried defect.

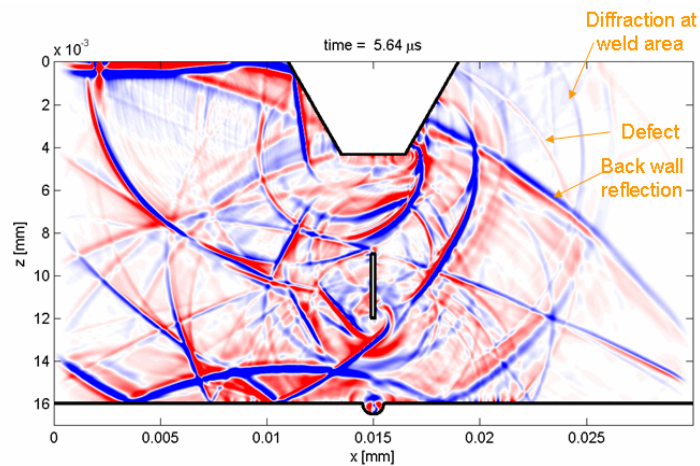


**Figure 14** Wavefront positions 5.64 us after laser generation, showing the cluttered arrival features at a position symmetrically opposite to the position of generation.

#### 6.4 Task 4: Phase I Project Administration and Reporting

All reports were submitted within 15 days of the end of the reporting period.

#### 6.5 Task 5: Integration for Remote Testing

##### 6.5.1 Integration Activities at IOS

The head is designed to mount on a rotating carriage that also supports the weld head (Figure 15). The head sits about 30 cm downstream from the weld region. Thus, we will be interrogating the completed weld 10-20 seconds after it is created, thereby insuring that the weld is solidified, with any potential defects already formed.

As shown in Figure 16, the ALUT head contains the generation laser head, so as to avoid delivering the generation laser beam through a fiber, with the associated risk of laser damage. The commercial generation laser is specifically designed to be hardened for industrial use. The probe and signal beams have a much lower damage risk, so they are delivered through a fiber bundle (not shown). The beams at the pipe surface are set to straddle the weld seam, with a nominal separation of 18 mm, as required for 1/2" wall pipe. For other values of pipe diameter, a remotely adjustable steering mirror can be used to modify the beam spacing. Figure 17 shows the measurement head with the cover attached.

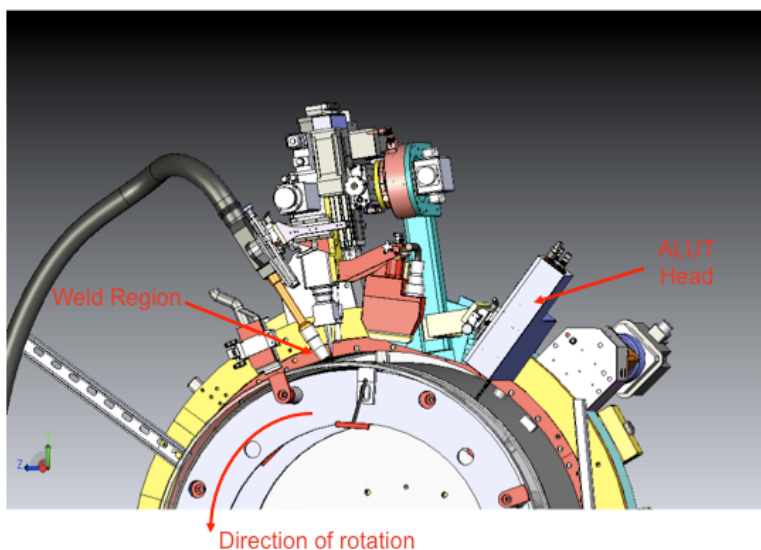


**Figure 15** SolidWorks image of the rotating carriage containing the weld head, the profiling camera and the ALUT head.

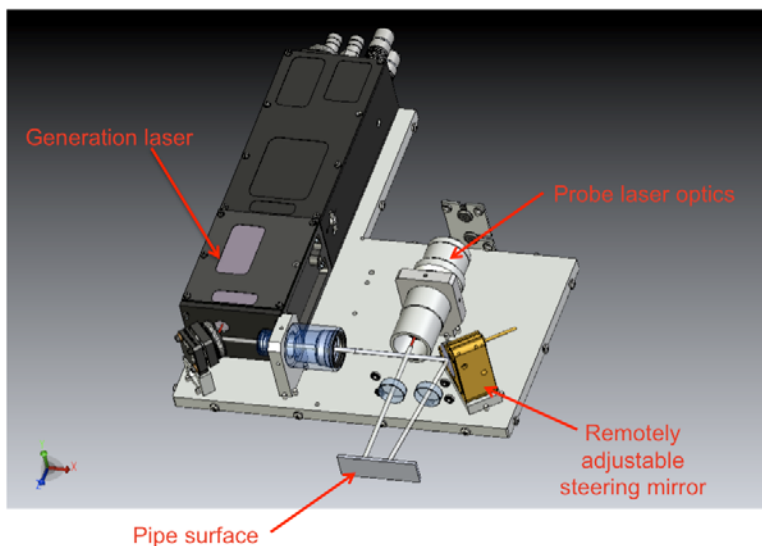


**Figure 16** SolidWorks image of the interior of the ALUT head, showing the generation laser and beam delivery optics.

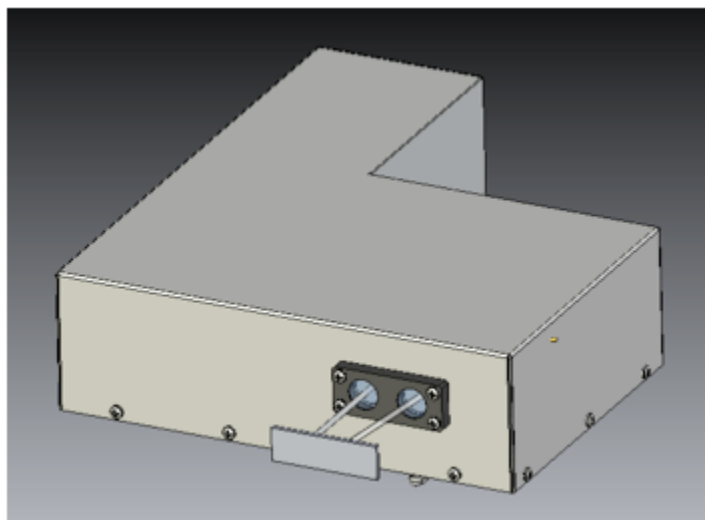


**Figure 17** Measurement head with cover, showing beams directed to pipe surface.

### 6.5.3 High Power Probe Laser Design Modified

During the demonstration at ATS, it was recognized that our 2W detection laser was insufficient for producing good detection signals on typical pipe surfaces. We worked with IPG Photonics to specify a fiber probe laser with sufficient power to interrogate all possible surfaces that may be encountered. The performance specifications are generic:

- Wavelength: 1550 nm
- Linewidth: 10 MHz
- Power: 10W
- Fiber type: single mode, unpolarized.

However, customization is required to integrate with other components in our system. First, the variable fiber splitter that we use is only rated to 2W average power. Thus, we asked IPG to add the capability to pulse the laser output. The laser only needs to be activated during signal

acquisition, which is no more than 50  $\mu$ s. The repetition rate is typically 20 Hz, so the duty cycle is only  $10^{-3}$ . Thus, 10W of peak laser power (during the pulse) corresponds to only 10 mW average power.

The laser we have specified has a significant requirement on return loss, to insure that feedback into the fiber amplifier does not lead to damage. In order to minimize this risk, we have asked IPG to add a second isolator at the laser output.

The high power and narrow linewidth from this laser place limitations on the length of the single mode fiber pigtail from the laser. In order to allow propagation over practical distances, we will couple from single mode into multimode fiber having a larger core diameter.

#### **6.5.4 Receiver Modifications Complete**

Our commercial AIR receivers use a photorefractive crystal as an adaptive beam combiner in a Mach-Zehnder interferometer. The real-time holographic gratings in the crystal act to compensate for low frequency mechanical noise from vibrations, and speckle motion from interrogating a moving surface. This compensation function is critical, as mechanical noise displacements can exceed 1 mm (at  $\sim$ 10 Hz), while the system is trying to detect 1 nm displacements at 10 MHz. The type of crystal currently in use does provide perfect compensation. For this reason, we have substituted a different crystal, which we believe will provide the desired improved performance.

### **6.6 Task 6: Evaluation and Qualification at BMT**

#### **6.6.1 Benchmarking against Phased Array UT**

ATS has provided a welded flat plate sample (ATS/Olympus #2) with a known centerline crack that was observed in a macro (Figure 18) taken toward the middle of the sample. A clear centerline crack is seen, and is expected to run through the whole sample. After cutting for the macro, two samples were generated (Figure 19), labeled Sample 1 and Sample 2. Both samples were sent to Olympus for inspection by phased array UT. The inspection results confirmed and identified the centerline crack extending completely through Sample 2 and partway through Sample 1. The measured depth was 7.9 mm, but no height in the through-wall direction could be obtained.

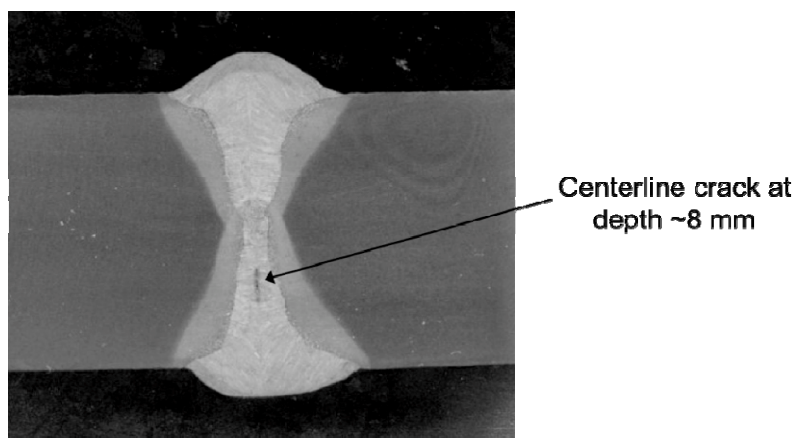


**Figure 18** Weld macro.

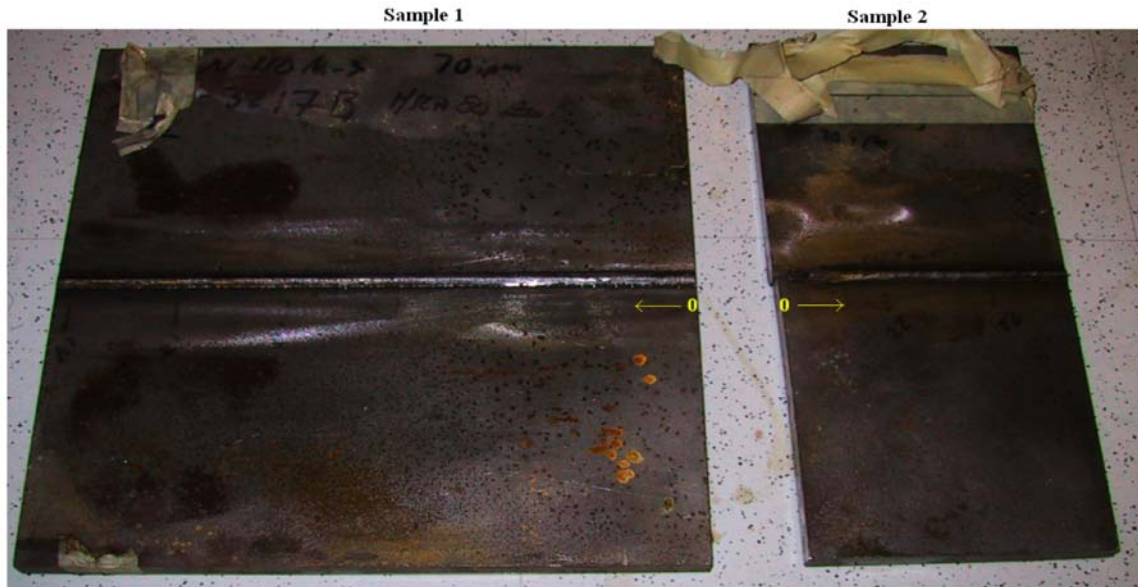


**Figure 19** Photo of ATS weld samples after cutting for macro purposes.

We have scanned Sample 2, using a beam separation of 18 mm. The rather large beam separation relative to the sample thickness means that transverse (shear) waves are favored over longitudinal waves. A typical B-scan (after processing) is shown in Figure 20. We have identified all the important arrivals. The centerline crack shown in Figure 19 is clearly seen as the wavy lines at an arrival of 8-9 us. This defect arrival represents shear wave scattering. On careful examination, there are two lines of varying amplitude that are separated by about 0.2-0.4 us. These separate arrivals are likely scattering from the top and from the bottom of the defect. The measured time difference allows a direct measurement of the defect height.

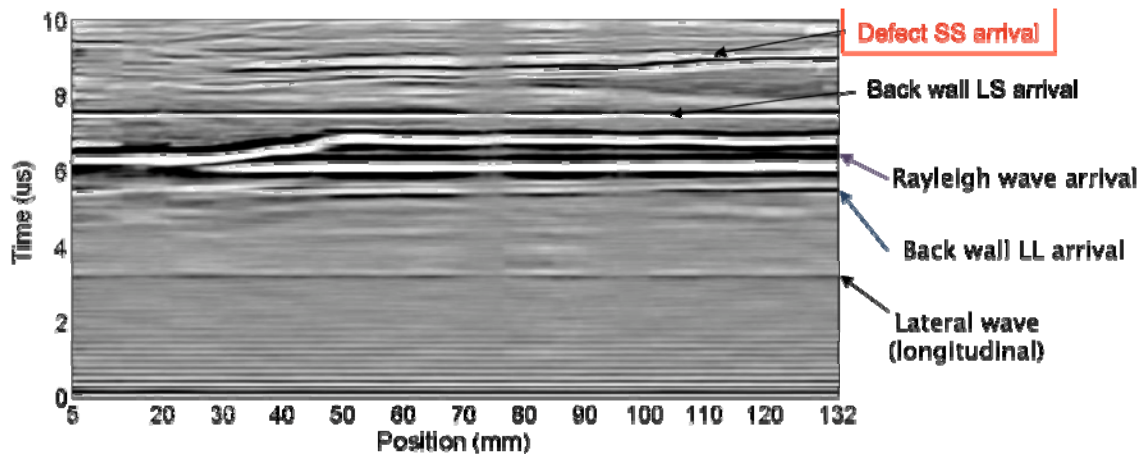


**Figure 20** B-scan of ATS/Olympus Sample #2, using a beam separation of 18 mm.

In summary, the Olympus measurements have confirmed the prominent centerline crack that we detected using laser ultrasonics. Our technique can go beyond the capabilities of Olympus in that we can measure the height of the defect.

### 6.6.2 Demo of ALUT System with HLAW Demo

The demo took place at ATS on May 28, 2009. The HLAW weld system and the ALUT system were integrated and demonstrated together.

The innovation in our ALUT system is associated with the design of the measurement head, which was shown in Figure 16. The detection subsystem consisted of an integrated (FHY) head that was modified for integration into the ALUT head. We used a lens with a focal length of 150 mm (instead of the normal 50 mm in our generic FHY) in this FHY so that we could stand off further from the surface and also provide a larger depth of focus. The equivalent collection f/number was f/6.

We did not fiber couple the generation beam into the measurement head. In order to obtain adequate signal levels, we need the full 50 mJ from our Ultra laser, which would require the use of a 1 mm core delivery fiber. The large core diameter would not allow focusing to a small enough spot on the pipe surface, nor would the depth of focus be adequate. Fortunately, the Ultra head is small, so we mounted the laser head directly inside the measurement head and fed water and power/controls through a long umbilical. An image of the measurement head with the cover attached was shown in Figure 17.

As shown in Figure 21, we designed the measurement head to be mounted onto the weld head carriage in a trailing position after the weld. Specifically, the ALUT head trails the weld by about 14 inches. For a typical weld speed of 40 mm/s, the pipe temperature at the point of inspection is quite low--approximately 300° C.

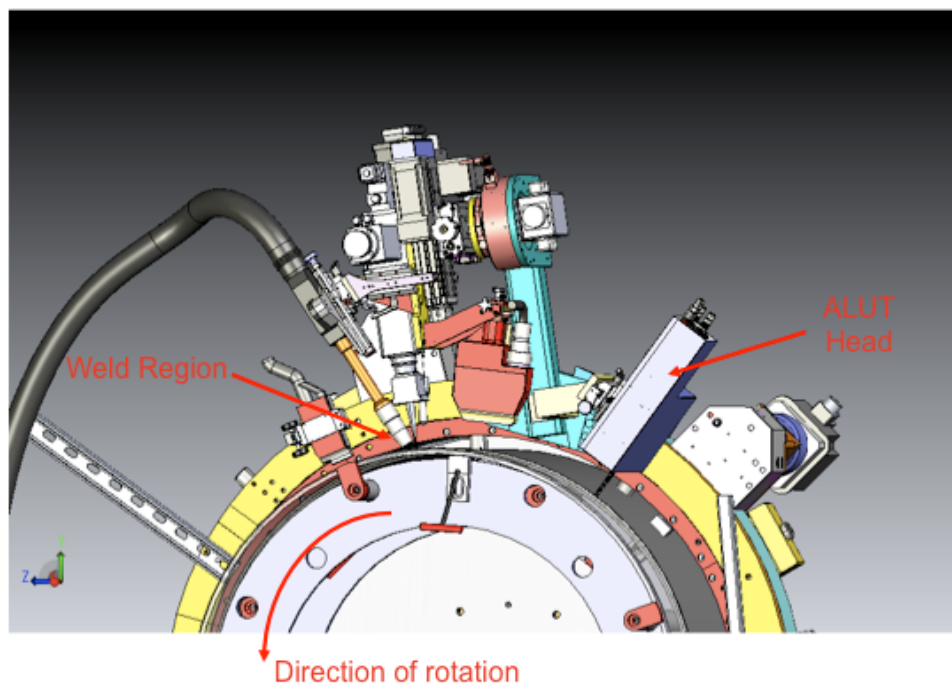


**Figure 21** Pipe weld setup, showing weld head and ALUT measurement head. Both heads and associated hardware rotate counter clockwise during welding.

Aside from the hardware integration shown in Figure 21, we also had to plan for software/controls integration with the weld controller. Our own acquisition/processing software was adapted from IOS commercial software (LaserScan) for data acquisition, processing and

display. By intention, ATS varies the weld speed during rotation around the pipe. To economize on resources, we simplified the acquisition by free running the generation laser, which provided a trigger to the acquisition software, without direct knowledge of the position along the weld. In other words, we were acquiring signals at equal time intervals that were not tied to their position on the pipe. We intended to control the start and stop of acquisition using a TTL-logic bit provided by the weld control computer, but there was too much electromagnetic interference in the environment, so the start/stop of acquisition was manually controlled instead.

Before shipment of the equipment to ATS, we assembled and ran the complete system at IOS. The system functioned as designed. We shipped 13 boxes of equipment to ATS. Integration of this equipment is a significant activity. As we unpacked and set up the equipment, we discovered a number of problems that were successfully debugged prior to the day of the demonstration.

The integration of the ALUT hardware (measurement head and support cables) onto the weld carriage proceeded smoothly. The mount provided by ATS mated to the base of the ALUT head. ATS provided mechanical slides for adjustment of standoff and lateral position relative to the weld seam. Once the slides were locked, the head was quite stable. Figure 22 is a photo of the entire setup and Figures 23-24 show close-ups of the integrated ALUT measurement head.

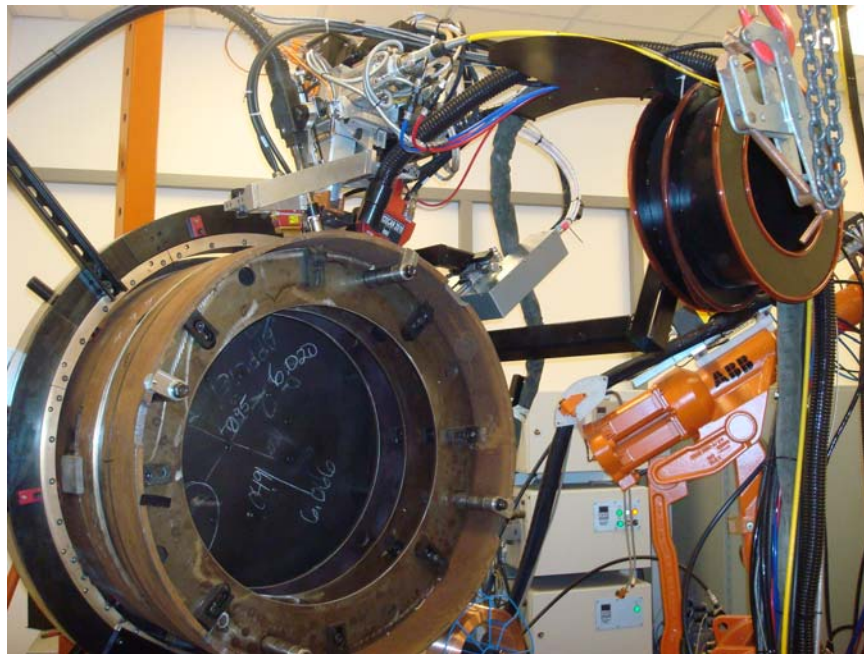


**Figure 22** Photo of weld setup, with ALUT measurement head in the center.



**Figure 23** Close-up of integrated measurement head from rear.



**Figure 24** Close-up of integrated measurement head from front.

We designed the ALUT head to be nominally sealed, but there were small openings for the generation laser umbilical (Figure 23) and the fiber bundle for the detection optics. In order to limit infiltration of dust into the interior, the design included a provision for positive pressurization using clean air or nitrogen. The clean nitrogen hose provided by ATS was larger than the fitting we provided. ATS modified the fitting for their hose, but in the end we did not use any gas pressurization, as we felt the delivery pressure was too high, and we did not want to risk any surprises. In the time we operated, neither the outside windows nor the interior of the head showed signs of dust. On the other hand, our support equipment did become quite dirty over the three days it was set up on a table in the weld cell.

With our head in place and set at the optimum focus/standoff, we ran a scanning test in which no welding was performed, but the carriage was rotated at the normal weld speed. Beforehand, we translated the weld head so the two beams were both on one side of the weld seam. During the scan, we thus would expect to see a Rayleigh wave and a back wall echo. The data acquisition worked well, but the B-scan was very noisy, with only a weak Rayleigh wave and no obvious back wall reflection.

We collected two scans during welding. In both cases, the signal-to-noise in the B-scans was less than desirable. As a result, we decided to purchase a more powerful laser, and to switch to a new crystal in our receiver.

### **6.7 Task 7: Develop Final System Specification**

Based on our experience in this project, we are in a position to provide a system specification for an end user, as well as a technical specification for the specialist. These apply to the ALUT subsystem that will be integrated into the weld head, as done for the HLAW demo. The specifications are given as:

#### **System Specifications (assume a weld speed of 1.8 m/minute)**

- Measurement rate: 20 measurements/second
- Measurement spacing along weld: 1.5 mm
- Minimum detectable defect length along weld: 3 cm
- Minimum detectable through-wall height of defect: 1 mm
- User data display: B-scan taken along the weld (same as used for current AUT).

#### **Technical Specifications**

- Generation laser wavelength: 1064 nm
- Generation laser energy: 50 mJ/pulse
- Generation laser repetition rate: 20 pulses/second
- Detection laser wavelength: 1550 nm
- Detection laser power: 10 watts
- Measurement head distance from weld head: 30 cm or more
- Measurement head standoff: 120 mm
- Measurement head depth of focus: +/-8 mm
- High-low tolerance: +/-4 mm.

### **6.8 Task 8: Update ROI Analysis**

This ROI is defined as the ratio of (a) the discounted cost avoidance realized by the proposed manufacturing methods over 5 years, to (b) the equipment and implementation costs for the proposed processing method. Modifications to this standard definition are included to account for (1) the funds required to implement an automated laser ultrasonic testing system, including labor, material, equipment costs, and (2) a phase-in period in which first year savings are based on partial use of the new system.

An alternate and simpler measure of economic benefit is a payback analysis, in which the number of years required for cost savings to balance initial capital and implementation costs is calculated. This is the approach we will take here.

To perform our payback calculation, we consider two types of installations: in-line, real-time process control and off-line inspection. The economic benefits of each for a single installation and the associated cost savings are given below.

#### **Real Time Process Control**

Early detection of defects and the resulting real-time correction of the process will eliminate post-process inspection costs and produce fewer defects in the finished weld, and thus reduce repair costs.

Calculation of cost savings due to elimination of post-process inspection:

- Inspector work load: 16 hours/day, 250 days/year
- Inspector cost: 4000 hours/year at \$40/hour, for a total of \$160,000/year

Calculation of cost savings due to reduced repairs:

- Weld rate: 80 joints/day or 20,000 joints/year
- Percentage of joints that currently need repair: 1% or 200 repairs/year
- Number of repairs using ALUT system: 20 repairs/year
- Repair savings: 180 repairs/year that would require 900 man-hours at \$40/hour, or \$36,000/year

Total cost savings per installation per year: \$196,000

Estimated cost of single installation: \$250,000

Payback period: 15 months

### **Off-line Inspection**

ALUT could be used off-line as a replacement for more labor-intensive inspection techniques now in use.

From the above calculation:

Total cost savings per installation per year: \$160,000.

Estimated cost of a single installation: \$200,000.

Payback period: 15 months

## **6.9 Task 9: Phase II Project Administration and Reporting**

All reports were submitted within 15 days of the end of the reporting period.

## **7.0 CONCLUSIONS**

In this project we have developed a rugged system for the in-line, automated inspection of hybrid laser/arc girth welds used in pipeline assembly. Lab measurements showed that typical weld defects could be detected and displayed. Our system was demonstrated to industry specialists as part of a demonstration of the HLAW system. The system operated according to specifications, and acquired data in real time during the weld process. Future work would focus on hardening the system for field use, and also on fully automating the software.

## ATTACHMENT 2

### Summary Project Financials

The following table provides a summary of the financial status for the project:

Actual costs for all participants Quarter 10					Cash cost share Quarter 10					In kind cost share Quarter 10							
Milest one No.	Task	Budgeted milestone payments	Cumulative budgeted payments	Costs incurred	Cumulative costs incurred	Milest one No.	Task	Forecast	Received	Total cash share forecast	Total Cost Share Received	Milest one No.	Task	Forecast	Received	Total In Kind cost share forecast	Total In Kind Cost Share Received
1	1	64,298.00	64,298.00	64,298.00	64,298.00	1	1	43,634.00	43,634.00	43,634.00	43,634.00	1	1	20,664.00	20,664.00	20,664.00	20,664.00
2	1	70,122.00	134,420.00	70,122.00	134,420.00	2	1	47,122.00	47,122.00	47,122.00	47,122.00	2	1	23,000.00	23,000.00	23,000.00	23,000.00
3	1	126,402.00	260,822.00	126,402.00	260,822.00	3	1	71,402.00	71,402.00	71,402.00	71,402.00	3	1	55,000.00	55,000.00	55,000.00	55,000.00
4	4	2,557.00	263,379.00	2,557.00	263,379.00	4	4	2,557.00	2,557.00	2,557.00	2,557.00	4	4	0.00	0.00	-	0.00
5	2	114,155.00	377,534.00	114,155.00	377,534.00	5	2	55,155.00	55,155.00	55,155.00	55,155.00	5	2	59,000.00	59,000.00	59,000.00	59,000.00
6	2	132,715.00	510,249.00	132,715.00	510,249.00	6	2	65,215.00	65,215.00	65,215.00	65,215.00	6	2	67,500.00	67,500.00	67,500.00	67,500.00
7	2	90,942.00	601,191.00	90,942.00	601,191.00	7	2	35,442.00	35,442.00	35,442.00	35,442.00	7	2	55,500.00	55,500.00	55,500.00	55,500.00
8	4	2,557.00	603,748.00	2,557.00	603,748.00	8	4	2,557.00	2,557.00	2,557.00	2,557.00	8	4	0.00	0.00	-	0.00
9	3	39,555.00	643,303.00	39,555.00	643,303.00	9	3	18,055.00	18,055.00	18,055.00	18,055.00	9	3	21,500.00	21,500.00	21,500.00	21,500.00
10	3	34,387.00	677,690.00	34,387.00	677,690.00	10	3	12,887.00	12,887.00	12,887.00	12,887.00	10	3	21,500.00	21,500.00	21,500.00	21,500.00
11	3	28,133.00	705,823.00	28,133.00	705,823.00	11	3	6,633.00	6,633.00	6,633.00	6,633.00	11	3	21,500.00	21,500.00	21,500.00	21,500.00
12	4	2,557.00	708,380.00	2,557.00	708,380.00	12	4	2,557.00	2,557.00	2,557.00	2,557.00	12	4	0.00	0.00	-	0.00
13	5	43,278.00	751,658.00	43,278.00	751,658.00	13	5	14,355.00	14,355.00	14,355.00	14,355.00	13	5	28,923.00	28,923.00	28,923.00	28,923.00
14	9	4,127.00	755,785.00	4,127.00	755,785.00	14	9	4,127.00	4,127.00	4,127.00	4,127.00	14	9	0.00	0.00	-	0.00
15	5	35,385.00	791,170.00	35,385.00	791,170.00	15	5	14,885.00	14,885.00	14,885.00	14,885.00	15	5	20,500.00	20,500.00	20,500.00	20,500.00
16	9	4,127.00	795,297.00	4,127.00	795,297.00	16	9	4,127.00	4,127.00	4,127.00	4,127.00	16	9	0.00	0.00	-	0.00
17	5	35,274.00	830,571.00	35,274.00	830,571.00	17	5	14,774.00	14,774.00	14,774.00	14,774.00	17	5	20,500.00	20,500.00	20,500.00	20,500.00
18	5	34,350.00	864,921.00	34,350.00	864,921.00	18	5	15,350.00	15,350.00	15,350.00	15,350.00	18	5	19,000.00	19,000.00	19,000.00	19,000.00
19	9	0.00	864,921.00	0.00	864,921.00	19	9	0.00	0.00	0.00	0.00	19	9	0.00	0.00	-	0.00
20	6	75,286.00	940,207.00	75,286.00	940,207.00	20	6	37,286.00	37,286.00	37,286.00	37,286.00	20	6	38,000.00	38,000.00	38,000.00	38,000.00
21	6	34,400.00	974,607.00	34,400.00	974,607.00	21	6	11,900.00	11,900.00	11,900.00	11,900.00	21	6	22,500.00	22,500.00	22,500.00	22,500.00
22	9	0.00	974,607.00	0.00	974,607.00	22	9	0.00	0.00	0.00	0.00	22	9	0.00	0.00	-	0.00
23	5	85,000.00	1,059,607.00	85,000.00	1,059,607.00	23	5	25,000.00	25,000.00	25,000.00	25,000.00	23	5	60,000.00	60,000.00	60,000.00	60,000.00
24	5	25,000.00	1,084,607.00	25,000.00	1,084,607.00	24	5	25,000.00	25,000.00	25,000.00	25,000.00	24	5	0.00	0.00	-	0.00
25	5	40,000.00	1,124,607.00	40,000.00	1,124,607.00	25	5	25,000.00	25,000.00	25,000.00	25,000.00	25	5	15,000.00	15,000.00	15,000.00	15,000.00
26	9	0.00	1,124,607.00	0.00	1,124,607.00	26	9	0.00	0.00	0.00	0.00	26	9	0.00	0.00	-	0.00
27	7	18,751.00	1,143,358.00	18,751.00	1,143,358.00	27	7	10,251.00	10,251.00	10,251.00	10,251.00	27	7	8,500.00	8,500.00	8,500.00	8,500.00
28	8	15,477.00	1,158,835.00	15,477.00	1,158,835.00	28	8	9,977.00	9,977.00	9,977.00	9,977.00	28	8	5,500.00	5,500.00	5,500.00	5,500.00
29	9	0.00	1,158,835.00	0.00	1,158,835.00	29	9	0.00	0.00	0.00	0.00	29	9	0.00	0.00	-	0.00
30	9	11,200.00	1,170,035.00	11,200.00	1,170,035.00	30	9	7,700.00	7,700.00	7,700.00	7,700.00	30	9	3,500.00	3,500.00	3,500.00	3,500.00
31	9	0.00	1,170,035.00	0.00	1,170,035.00	31	9	0.00	0.00	0.00	0.00	31	9	0.00	0.00	-	0.00
32	n/a	2,000.00	1,172,035.00	2,000.00	1,172,035.00	32	n/a	2,000.00	2,000.00	2,000.00	2,000.00	32	n/a	0.00	0.00	-	0.00